Chapter 3. The Two-Dimensional Forward Problem

Introduction

In this section we will relax the one-dimensional assumption made earlier and consider a two-dimensional model of the subsurface. As before, we will choose to neglect shear waves and absorption of the waves.

Under these comparatively modest restrictions the scalar wave equation completely describes the behavior of the seismic wave fields. In addition to primary reflections, implicit in the wave equation are the predicted effects of geometrical spreading, moveout, diffraction, and multiple reflections. Through finite difference solutions to the wave equation we shall model these phenomena, paying particular attention to diffracted multiple reflections.

The impetus for simulating the reflection problem with the wave equation stems largely from observations of field data. Diffraction hyperbolas and focused regions on the time section are common and distinguishing features of wave propagation. When they may be identified as primary reflections, the true shape of the reflector may be deduced through migration. Migration of primary reflected waves, either using the wave equation (Claerbout and Doherty, 1972) or geometrically (Peterson and Walter, 1974), is a well understood technique to the explorationist. The contribution of multiple reflected waves is less than well understood except in unusually ideal subsurface geometries. Their identification on field data usually relies on association of the diffraction features with undiffracted portions of the seafloor and pegleg multiples. More often though, the wave phenomena is less obvious. In one case, repeated focusing and defocusing on a rough seafloor leads to lateral incoherence in

the high order multiples. Depending on whether or not we choose to model this energy it is regarded as signal-generated-signal or signal-generated-noise. Whereas, on the other extreme, multiple reflections off a dipping surface leads to systematic shortening of the reverberation period. The virtue then, of wave equation simulation is that we include diffracted multiples as a physically deterministic or predicted part of our model rather than a statistical or systematic departure from it.

In this section we consider the forward problem, that is; given the 2-D spatial distribution of reflection coefficients, compute the reflected wave field observed at the earth's surface. We will first develop the equations for separately propagating up and downgoing waves, then the finite difference formulation for solving them in the computer, and finally, synthetic examples. In chapter 4 we will consider the practically important inverse problem, that of deducing the reflection coefficients from the waves.

Continuation Equations

To begin with, we will formulate the problem of simulating the wave equation in terms of upward and downward traveling waves. More precisely, we will separate the wave equation into two separate Partial Differential Equations (PDEs): one which describes the propagation of upcoming waves and another for downgoing waves. This is done for a number of different reasons, not among the least important is simply the conceptual aid of thinking in terms of up and downgoing waves. Secondly, by splitting the waves we may define local coordinate frames which propagate with the two solutions. For the reflection seismology geometry the propagation is generally collimated about vertical paths.

By perturbing the solution along such paths we reduce much of the pure translation the PDE has to do. It makes little sense to use a wave equation to move energy to a position which can approximately be predicted by a well-chosen coordinate frame. The pay-off of this practice comes in the ability to propagate a relatively large distance for the same cost as a small distance. Thirdly, by separating the wave fields the coupling between the two components becomes an explicit relationship. This coupling, defined by the reflection coefficients of the model, may be modified in order to selectively synthesize all or any of the classes of multiple reflections. Finally, and of primary importance, is that separation of the wave field into up and downgoing parts is of fundamental importance to the inverse calculation.

Thus, we are led to consider means of splitting the wave equation. Rather than attempt a rigorous mathematical separation, we will use a numerical technique due to Claerbout (1970). The method involves transforming the wave equation into a coordinate frame such that the waves of interest become slowly varying functions in one of the transformed coordinates. In such a frame the unwanted solution may be discriminated against by a low-pass filtering operation in the appropriate coordinate. Since we are interested in computing both solutions simultaneously yet separately, two transformations will be required.

In the field we record or sample the reflected wave field as a function of the profiling or in-line coordinate, x and time, t. To extrapolate the component solutions separately along the wave path we introduce two separate transformations of the time coordinate.

Normally the wave field is recorded at the earth's surface, but imagine a horizontal line of geophones positioned at some fixed depth along the z-axis. Referring to Figure 3-1, this location is chosen to be a short distance above a reflecting interface. Time in the frame at the left is referenced to the initiation of the surface disturbance. At some time after the shot we record the passage of the downgoing wave, D . A short time later we record the reflected upcoming wave, U . Such would be the observations in an absolute time frame. As the geophones were moved up toward the surface the two waves would diverge. D would end up at t=0 , while the primary reflection U would end up near the bottom of the frame.

The two transformations to the right attempt to predict this vertical translation based on the receiver depth, z and the wave speed $\bar{v}$. The new coordinate frames remain fixed in space relative to the absolute frame. However, time is now a function of position. In the center frame, when an observer moves in the -z direction time t will seem to go slower. Moving with precisely the wave speed time stands still. Thus, the same upcoming wave, as observed in the center frame, does not change very much as it travels up to the surface. It appears on the frame where z equals the depth to the reflector. When it appears is the two-way travel time we predict it will arrive at the surface. Likewise, in the frame at the right, when an observer (receiver) moves downward time will also seem to run slow. For a downgoing wave departing the surface at t=t"=0 it would remain near the top of the frame as it propagated downward. The earliest possible downgoing wave would be represented at t"=0 . Other waves departing the surface would appear on the frame at t"=t and remain in approximately that position.

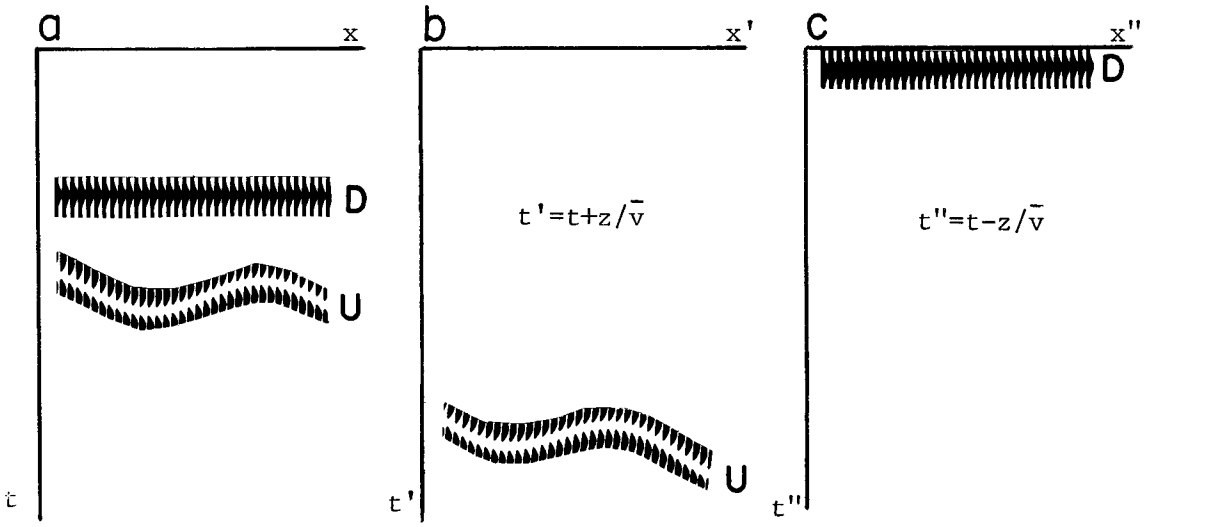

Figure 3-1. Time response at buried receivers due to a surface disturbance. For a horizontal line of receivers positioned a short distance above a reflector we first record the passage of the downgoing wave D. A short time later the reflected upcoming wave U is recorded. In the surface arrival frame the upcoming wave appears at the two-way travel time. In the surface departure frame the downgoing wave is at $t''=0$. As the receivers move up to the surface, U and D diverge in the fixed frame, but U and D remain stationary as viewed in their respective relative time frames.

These two frames appear, then, to be well suited for describing waves propagating at moderate angles to the vertical. The surface arrival (U) frame is good for upcoming waves, while the surface departure (D) frame is good for downgoing waves. The term "good" is directly related to the ability to extinguish the unwanted solution and model the desired solution. In the U-frame the upcoming wave energy is shifted toward $k_z'=0$, where k_z' is the vertical wavenumber measured in the transformed coordinates. Similarly, downgoing waves are shifted toward $k_z''=0$ in the D-frame. Waves in the opposing directions are conversely shifted to rapidly varying functions of z. On this basis, we may distinguish the waves of interest as shifted toward $k_z=0$ as measured in either frame.

The two-dimensional scalar wave equation in cartesian coordinates is

$$P_{xx} + P_{zz} - 1/\tilde{v}^2 P_{tt} = 0 \qquad (3\text{-}1)$$

With the wave equation in this form we are implicitly assuming that density gradients may be neglected compared to velocity variations. The upward (surface-arrival) transformation is given by

$$\begin{aligned} x' &= x \\ z' &= z \\ t' &= t + z/\bar{v} \end{aligned} \qquad (3\text{-}2\ a,b,c)$$

and the downward (surface-departure) transformation by

$$\begin{aligned} x'' &= x \\ z'' &= z \\ t'' &= t - z/\bar{v} \end{aligned} \qquad (3\text{-}3\ a,b,c)$$

The frame velocity $\bar{v}$ is initially taken to be constant. Once having settled on a particular coordinate transformation, or in this problem two transformations, the next step is to express the wave equation in the new coordinate frames. First we make the statement that the wave field is invariant under a coordinate transformation.

$$P(x, z, t) = U(x', z', t') = D(x'', z'', t'') \qquad (3\text{-}4)$$

Although equation (3-4) may seem paradoxical at first, in view of the fact that we are trying to separate the waves, at this point U and D merely represent different dependent transform variables. That is, we have the possibility of expressing the total wave field in either frame. Shortly we will make the numerical approximation which accomplishes the separation. We will first develop equations for propagating the separate solutions in homogeneous regions where, of course, they uncouple. Later the coupled equations for inhomogeneous regions will be developed.

First consider the upcoming transformation. The chain rule for differentiation, using equations (3-2), gives

$$\partial_{xx} P = \partial_{x'x'} U \qquad (3\text{-}5\ a)$$

$$\partial_{zz} P = (\partial_{z'z'} + 2/\bar{v}\ \partial_{t'z'} + 1/\bar{v}^2\ \partial_{t't'})\ U \qquad (3\text{-}5\ b)$$

$$\partial_{tt} P = \partial_{t't'} U \qquad (3\text{-}5\ c)$$

Inserting these into the wave equation yields

$$U_{x'x'} + U_{z'z'} + 2/\bar{v}\ U_{t'z'} + (1/\bar{v}^2 - 1/\tilde{v}^2)\ U_{t't'} = 0 \qquad (3\text{-}6)$$

Further, defining

$$\varepsilon(x', z') \triangleq (\bar{v}^2 / \tilde{v}(x',z')^2 - 1) \tag{3-7}$$

as a measure of the excursion of the medium velocity from the frame velocity, we have the wave equation expressed in upcoming coordinates.

$$U_{t'z'} = -\bar{v}/2\, U_{x'x'} + \varepsilon/2\bar{v}\, U_{t't'} - \bar{v}/2\, U_{z'z'} \tag{3-8}$$

In this frame the waves of interest are shifted toward zero vertical wavenumber. This is strictly true in homogeneous regions along vertical paths. Thus, to extinguish all downgoing waves in equation (3-8) we are led to drop the term proportional to $k_{z'}^2$, namely $U_{z'z'}$.

$$U_{t'z'} = -\bar{v}/2\, U_{x'x'} + \varepsilon/2\bar{v}\, U_{t't'} \tag{3-9}$$

Note that in dropping this term we have also implicitly set the transmission coefficient to unity. This is just as we require, since the waves exactly uncouple only in homogeneous media. When we later recouple the up and downgoing waves reflection and transmission coefficients will be included. A better approximation results if we use equation (3-9) as a trial solution from which we may estimate $U_{z'z'}$, for equation (3-8). Thus, integrating equation (3-9) over t'

$$U_{z'} = -\bar{v}/2\, U^{t'}_{x'x'} + \varepsilon/2\bar{v}\, U_{t'} \tag{3-10}$$

and differentiating with respect to z' we arrive at an estimate for $U_{z'z'}$ which is first order in z'.

$$U_{z'z'} = -\bar{v}/2\, U^{t'}_{x'x'z'} + \varepsilon_{z'}/2\bar{v}\, U_{t'} + \varepsilon/2\bar{v}\, U_{t'z'} \tag{3-11}$$

For uncoupled solutions we require that $\varepsilon_{z'} = 0$ (since ε = const for homogeneous media). Inserting equation (3-11) into equation (3-8) we obtain

$$(1 + \varepsilon/4) U_{t'z'} = - \bar{v}/2 \, U_{x'x'} + \bar{v}^2/4 \, U^{t'}_{x'x'z'} + \varepsilon/2\bar{v} \, U_{t't'} \qquad (3\text{-}12)$$

The new term, $U^{t'}_{x'x'z'}$, provides better accuracy in propagating off-axis ($\approx$ 1% relative velocity error at 45°) waves than equation (3-9). A discussion of this type of approximation may be found in Claerbout (1971a). The angular bandwidth we need consider is data dependent, i.e., upon the source/receiver geometry and the subsurface dip. Neglecting this term limits consideration to waves propagating within about 15° of the vertical axis, a narrow beam approximation.

Next, let's consider waves in the downgoing transformation of equations (3-3). Again using the chain rule,

$$\partial_{xx} P = \partial_{x''x''} D \qquad (3\text{-}13 a)$$

$$\partial_{zz} P = (\partial_{z''z''} - 2/\bar{v} \, \partial_{t''z''} + 1/\bar{v}^2 \, \partial_{t''t''}) D \qquad (3\text{-}13 b)$$

$$\partial_{tt} P = \partial_{t''t''} D \qquad (3\text{-}13 c)$$

Inserting these into the wave equation gives

$$D_{x''x''} + D_{z''z''} - 2/\bar{v} \, D_{t''z''} + (1/\bar{v}^2 - 1/\tilde{v}^2) D_{t''t''} = 0 \qquad (3\text{-}14)$$

or

$$D_{t''z''} = \bar{v}/2 \, D_{x''x''} - \varepsilon/2\bar{v} \, D_{t''t''} + \bar{v}/2 \, D_{z''z''} \; . \qquad (3\text{-}15)$$

Now, dropping $D_{z''z''}$ will have the desirable effect of extinguishing all upcoming solutions, whereupon equation (3-15) becomes

$$D_{t''z''} = \bar{v}/2 \, D_{x''x''} - \varepsilon/2\bar{v} \, D_{t''t''} \qquad (3\text{-}16)$$

a first order equation in z'' for propagating downgoing waves. A similar equation to (3-12) may likewise be derived from the estimate

$$D_{z''z''} = \bar{v}/2 \, D^{t''}_{x''x''z''} - \varepsilon/2\bar{v} \, D_{t''z''} - \varepsilon_{z''} / 2\bar{v} \, D_{t''} \quad . \tag{3-17}$$

Again, to obtain the uncoupled downgoing solution, set $\varepsilon_{z''} = 0$ and insert (3-17) into equation (3-15).

$$(1 + \varepsilon/4) \, D_{t''z''} = + \bar{v}/2 \, D_{x''x''} + \bar{v}^2/4 \, D^{t''}_{x''x''z''} - \varepsilon/2\bar{v} \, D_{t''t''} \tag{3-18}$$

Thus, we have a pair of equations (3-12, 3-18) for upward and downward continuation of the separate uncoupled wave fields. In cases where the narrow-beam approximation holds we may use for upward and downward continuation

$$(1 + \varepsilon/4) \, U_{t'z'} = - \bar{v}/2 \, U_{x'x'} + \varepsilon/2\bar{v} \, U_{t't'} \tag{3-19a}$$

$$(1 + \varepsilon/4) \, D_{t''z''} = + \bar{v}/2 \, D_{x''x''} - \varepsilon/2\bar{v} \, D_{t''t''} \tag{3-19b}$$

Reflected Waves

Having developed continuation equations for separately computing up and downgoing waves in homogeneous regions, we now face the interesting prospect of including inhomogeneities. In arriving at equations (3-19 a,b) all possible reflections were suppressed in our effort to separate the solution. However, where reflectors exist the waves are coupled. Furthermore, their superposition at every point in time and space must equal the total wave field in our original wave equation. That is, now making the statement

$$P(x, z, t) = U(x', z', t') + D(x'', z'', t'') \qquad (3\text{-}20)$$

is equivalent to coupling the up and downgoing solutions. The procedure is to express the total field, composed of $U + D$, in the relative time frames, then identify and subtract the homogeneous solution for the oppositely traveling wave. This will leave the transmitted and reflected waves for one-way propagation.

Consider first the upcoming transformation from equations (3-2 c) and (3-3 c) we have $t''=t'-2z'/\bar{v}$. Through the description (3-2) we transform the waves

$$P(x, z, t) = U(x', z', t') + D(x', z', t'-2z'/\bar{v}) \qquad (3\text{-}21)$$

in the wave equation to upcoming coordinates, which after carefully keeping track of the independent variables, results in

$$[U(t') + D(t'-2z'/\bar{v})]_{t'z'} + \bar{v}/2[U(t')- D(t'-2z'/\bar{v})]_{x'x'} \qquad (3\text{-}22)$$

$$- \varepsilon /2\bar{v}[U(t')- D(t'-2z'/\bar{v})]_{t't'} + \bar{v}/2[U(t')-D(t'-2z/\bar{v})]_{z'z'} = 0$$

The time dependence has been explicitly written to emphasize the shift that must occur in computing a downgoing solution on an upcoming frame. Equation (3-22) contains both up and downgoing reflected and transmitted waves. If we simply subtract off the homogeneous equation for the downgoing wave [equation (3-18)] we will leave the reflected, inhomogeneous, contribution of the downgoing energy. Doing this we have

$$U_{t''z''}(t') + \bar{v}/2\, U_{x'x'}(t') - \varepsilon/2\bar{v}\, U_{t't'}(t') + \bar{v}/2\, U_{z'z'}(t') = \tag{3-23}$$

$$\bar{v}/2\, D_{z'z'}(t'-2z'/\bar{v}) + \varepsilon/4\, D_{t'z'}(t'-2z'/\bar{v}) - \bar{v}^2/4\, D^{t'}_{x'x'z'}(t'-2z'/\bar{v})$$

The right hand side, using the previously derived estimate for $D_{z'z'}$ of equation (3-17), reduces to $-\varepsilon_{z'}/4\ D_{t'}(t'-2z'/\bar{v})$. Further, using the previous estimate for $U_{z'z'}$, equation (3-23) becomes

$$(1 + \varepsilon/4)\, U_{t'z'}(t') = -\bar{v}/2\, U_{x'x'}(t') + \bar{v}^2/4\, U^{t'}_{x'x'z'}(t') + \varepsilon/2\bar{v}\, U_{t't'}(t')$$

$$- \varepsilon_{z'}/4[\, U_{t'}(t') + D_{t'}(\, t' - 2z'/\bar{v}\,)] \tag{3-24}$$

Thus, we have an equation for propagating the upcoming waves through inhomogeneous regions. Comparing equation (3-24) to (3-12) we see that the inhomogeneous contributions are an upward reflected downgoing wave, $-\varepsilon_{z'}/4\, D_{t'}(\, t' - 2z'/\bar{v}\,)$, and a transmission effect $-\varepsilon_{z'}/4\, U_{t'}(t')$ on the upcoming wave.

Similarly, the downgoing solution may be computed by inserting the composite wave

$$P(\, x,\, z,\, t\,) = U(x'',\, z'',\, t'' + 2z''/\bar{v}\,) + D(\, x'',\, z'',\, t''\,) \tag{3-25}$$

into the downgoing transformation of equations (3-3) to give the

wave equation

$$[\, D(t'') + U(t''+2z''/\bar{v})]_{z''t''} - \bar{v}/2\, [\, D(t'') - U(t''+2z''/\bar{v})]_{x''x''} + \varepsilon/2\bar{v}\, [\, D(t'') - U(t''+2z''/\bar{v})]_{t''t''} - \bar{v}/2\, [\, D(t'') - U(t''+2z''/\bar{v})]_{z''z''} = 0 \,. \tag{3-26}$$

Again, subtracting off the homogeneous equation for the upcoming wave [equation (3-19 a)], and using the estimates (3-10) and (3-17), leaves the inhomogeneous downgoing equation

$$(1+\varepsilon/4)\, D_{t''z''}(t'') = \bar{v}/2\, D_{x''x''}(t'') + \bar{v}^2/4\, D^{t''}_{x''x''z''}(t'') - \varepsilon/2\bar{v}\, D_{t''t''}(t'') - \varepsilon_{z''}/4\, [\, D_{t''}(t'') + U_{t''}(\, t'' + 2z''/\bar{v}\,)\,] \tag{3-27}$$

The inhomogeneous source terms are the downward reflection of the upcoming wave, $-\varepsilon_{z''}/4\, U_{t''}(t'' + 2z''/\bar{v})$, and the downgoing transmission loss, $-\varepsilon_{z''}/4\, D_{t''}(t'')$. The narrow-beam equivalents to equations (3-24) and (3-27) are

$$(1+\varepsilon/4)\, U_{t'z'}(t') = -\bar{v}/2\, U_{x'x'}(t') + \varepsilon/2\bar{v}\, U_{t't'}(t') - \varepsilon_{z'}/4\, [\, U_{t'}(t') + D_{t'}(t'-2z'/\bar{v})\,] \tag{3-28 a}$$

$$(1+\varepsilon/4)\, D_{t''z''}(t'') = +\bar{v}/2\, D_{x''x''}(t'') - \varepsilon/2\bar{v}\, D_{t''t''}(t'') - \varepsilon_{z''}/4\, [\, D_{t''}(t'') + U_{t''}(t''+2z''/\bar{v})\,] \tag{3-28 b}$$

As a final simplification, consider letting the frame velocity $\bar{v}$ vary spatially. When $\bar{v}$ approaches $\tilde{v}(x,z)$ the correction term ∂_{tt} vanishes as does the correction $(1+\varepsilon/4)$ to the diffraction velocity. Expressing the z-derivative of equation (3-7) in terms of a velocity derivative yields

$$- \varepsilon_z/4 \;=\; - 1/4 \; \partial_z \left(\bar{v}^2/\tilde{v}^2(x,z) \;- 1 \right) = \frac{\bar{v}^2 \tilde{v}_z}{2\,\tilde{v}^3}$$

or

$$- \varepsilon_z/4 \;=\; (1 + \varepsilon)\; \tilde{v}_z \,/\, 2\tilde{v} \quad . \tag{3-29}$$

Thus, letting $\bar{v} = \tilde{v}(x,z)$ the excursion, ε , vanishes and equations (3-28) may be rewritten, dropping the primes on x and z , as

$$U_{t',z}(t') = -\tilde{v}/2 \; U_{xx}(t') + \tilde{v}_z/2\tilde{v}[\; U_{t'}(t') + D_{t'}(\; t' - 2z/\tilde{v} \;)] \tag{3-30 a}$$

$$D_{t'',z}(t'') = +\tilde{v}/2 \; D_{xx}(t'') + \tilde{v}_z/2\tilde{v}[\; D_{t''}(t'') + U_{t''}(\; t'' + 2z/\tilde{v} \;)] \tag{3-30 b}$$

The final result is a pair of coupled equations for propagating the separate solutions through velocity inhomogeneous regions. The coupling is now an explicit relationship prescribed by the vertical velocity gradient.

Transmission Losses and Intrabed Multiples

In the previous section equations for propagating the coupled up and downgoing wave fields were obtained including both reflection and transmission coefficients. Appending the appropriate initial value and boundary conditions specifies the problem for simulating surface reflection seismograms from complex reflector models. However, in many situations of practical interest we may choose to make additional simplification of the problem statement.

The first aspect concerns the inclusion of transmission coefficient effects in the finite difference calculations. Initially consider a layered, one-dimensional reflector model. For plane waves passing through plane layers conservation of energy yields a round-trip transmission loss factor of $\prod_{i=1}^{N} (1 - c_i^2)$ where c_i is the reflection coefficient of the i^{th} interface. The amplitudes we may expect to see at the surface (due to direct transmission to a particular reflector and back) is therefore a monotonically decreasing function of travel time which is independent of frequency. Calculations made without including transmission coefficients should be qualitatively similar to calculations including the loss. Quantitatively, the adjustment to amplitudes is then a simple positive scale factor dependent on travel time. In the forward problem we are given the reflection coefficients and may directly compute the scaling function to model transmission losses.

However, the interesting point is that the relationship between the primary and corresponding multiple reflected wave amplitudes is not altered by neglecting the transmission coefficients. This becomes important in approaching the inverse problem of trying to predict and

subtract multiple reflections utilizing relative amplitude information. This was illustrated in the example of the 1-D algorithm which was derived without reference to transmission effects. For a strictly one-dimensional geometry the transmission coefficients are unimportant in modelling and inverting multiples. We may expect that in somewhat less restrictive geometries the error associated with excluding transmission losses in the calculation may be negligible. Clearly, in modelling seafloor multiples transmission effects are zero. In those cases where the transmission coefficients are important, the transmission terms in equations (3-30) may be simply included by the finite difference method of the following section. This results in a slightly more complicated algorithm but adds little cost to the computations. In the subsequent numerical development the transmission terms in both equations (3-30a) and (3-30b) will be dropped.

Additionally, we may choose to neglect the very-long-delay intrabed multiples on the basis of amplitude. This is particularly appropriate for modeling marine data where a disturbingly large amount of multiple energy arises from reflections involving the sea surface and seafloor. For a seafloor of reflectivity ε_1 and a typical major interface with reflection coefficient ε_2 (where $\varepsilon_1 > \varepsilon_2$ and commonly $\varepsilon_1 >> \varepsilon_2$) we may rank in order of decreasing amplitude the classes of multiples:

-- seafloor peglegs	$0\ (\ n\,\varepsilon_1^{n-1}\,\varepsilon_2)$	big
-- seafloor multiples	$0\ (\ \varepsilon_1^{n}\ )$	↓ amplitude
-- structure-structure	$0\ (\ \varepsilon_2^{n}\ )$	
-- long-delay intrabed	$0\ (\ \varepsilon_2^{2n-1}\ )$	small

where the order, n represents the multiplicity of paths. With the belief that long-delay intrabeds are of negligible amplitude relative to seafloor multiples and seafloor peglegs, we will omit them from the calculation.

Since the coupling between the up and downgoing waves in equations (3-30) is explicit, the modification suggested above is easily accomplished by dropping the $\tilde{v}_z/2\tilde{v}\ U_{t''}$ term in equation (3-30 b). Of course the upcoming waves remain coupled onto the downgoing equation at the free surface. This will be handled separately by the boundary condition at the free surface, $z=0$. Thus, neglecting long-delay intrabed multiples and direct transmission losses we have the following initial-boundary value problem:

D.E.

$$U_{t'z}(x,z,t') = -\tilde{v}/2\ U_{xx}(x,z,t') + \tilde{v}_z/2\tilde{v}\ D_{t'}(x,z,t'-2z/\tilde{v}) \qquad (3\text{-}31\ a)$$

$$0 < z < \tilde{v}\ t'$$

$$D_{t''z}(x, z, t'') = \tilde{v}/2\ D_{xx}(x, z, t'') \qquad (3\text{-}31\ b)$$

$$z,\ t'' > 0$$

B.C.

$$D(x, z=0, t''=t) = -U(x, z=0, t'=t) \qquad (3\text{-}31\ c)$$

$$t > 0$$

$$R(x, t) = U(x, z=0, t'=t) \qquad (3\text{-}31\ d)$$

I.C.

$$U(x, z, t' \leqslant z/\tilde{v}) = 0 \qquad (3\text{-}31\ e)$$

$$D(x, z=0, t''=0) = E(x) \qquad (3\text{-}31\ f)$$

where the two-dimensional reflection seismogram $R(x,t)$ is defined as the upcoming wave observed at the surface, and $E(x)$ is the initial distribution of the surface explosion. Thus, given the surface shot geometry and the two-dimensional distribution of reflectors defined by $\tilde{v}_z(x,z) / 2\tilde{v}(x,z)$ equations (3-31) provide the mathematical description of the forward procedure for developing the reflection seismogram $R(x,t)$.

Finite Difference Formulation

Through finite difference approximations to the partial differential equations (3-31 a) and (3-31 b) we shall develop an algorithm for obtaining the up and downgoing wave solutions in velocity inhomogeneous media. The particular finite difference scheme to be used will be analogous to that of Crank-Nicholson. Let us discretize the coordinates as follows:

$x = j\,\Delta x$, $z = k\,\Delta z$, $t' = n'\,\Delta t$, and $t'' = n''\,\Delta t$;

(j, k, n', n'' integers) such that $U(x,z,t') = U(j\Delta x, k\Delta x, n'\Delta t)$

Thus, we denote the approximations to

$U(x, z, t')$ as $U^{n'}_{k,j}$ and to $D(x, z, t'')$ as $D^{n''}_{k,j}$

Throughout the following, the convention will be that when any index is absent the reference is to all values along the implied coordinate.

Defining the unit-delay operator $Z = e^{-i\omega\Delta t}$ and also the unit-shift operator $W = e^{-ik_z\Delta z}$ simplifies the difference notation. That is,

$$Z\,U^{n}_{k,j} = U^{n-1}_{k,j} \quad \text{and} \quad W\,U^{n}_{k,j} = U^{n}_{k-1,j} \ .$$

The centered finite difference approximations to the first derivatives are

$$\partial_z \simeq \frac{\delta_z}{\Delta z} = \frac{2}{\Delta z}\,\frac{(1-W)}{(1+W)} \qquad (3\text{-}32\ a)$$

$$\partial_t \simeq \frac{\delta_t}{\Delta t} = \frac{2}{\Delta t}\,\frac{(1-Z)}{(1+Z)} \qquad (3\text{-}32\ b)$$

and for second differencing in x

$$\partial_{xx} U \simeq \frac{\delta_x^2}{(\Delta x)^2} U^n_{k,j} = \frac{U^n_{k,j-1} - 2 U^n_{k,j} + U^n_{k,j+1}}{(\Delta x)^2} \qquad (3\text{-}32\ c)$$

The velocity gradient is approximated by

$$\frac{\delta_z \tilde{v}(x,z)}{2\,\tilde{v}(x,z)} \approx \frac{\delta_z \tilde{v}}{2\,\Delta z\,\tilde{v}} = \frac{[\tilde{v}(x,z) - \tilde{v}(x,z-\Delta z)]}{\Delta z[\tilde{v}(x,z) + \tilde{v}(x,z-\Delta z)]} \qquad (3\text{-}33)$$

From which we are led to define the constant density reflection coefficient, C , as

$$C(x,z) \triangleq \frac{\delta_z \tilde{v}}{2\,\tilde{v}} = \frac{[\,\tilde{v}(x,z) - \tilde{v}(x,z-\Delta z)\,]}{[\,\tilde{v}(x,z) + \tilde{v}(x,z-\Delta z)\,]} \qquad (3\text{-}34)$$

Thus, the model is represented as $C_{k,j}$ in index notation. Using the finite difference approximations of (3-32 a, b, c) and (3-34) we obtain the discrete form of the upcoming equation (3-31 a).

$$\frac{\delta_z}{\Delta z}\frac{\delta_{t'}}{\Delta t} U^{n'}_{k,j} = -\frac{\tilde{v}}{2(\Delta x)^2}\delta_x^2 U^{n'}_{k,j} + \frac{C_{k,j}}{\Delta z \Delta t}\delta_{t'} D^{n'-2k\Delta z/\tilde{v}\Delta t}_{k,j} \qquad (3\text{-}35)$$

Letting $\Delta z = \frac{\tilde{v}\,\Delta t}{2}$ and $a = \frac{\tilde{v}\,\Delta z \Delta t}{8(\Delta x)^2}$ we obtain

$$\frac{(1-Z)(1-W)}{(1+Z)(1+W)} U^{n'}_{k,j} = -a\,\delta_x^2 U^{n'}_{k,j} + 1/2\, C_{k,j}\frac{(1-Z)}{(1+Z)} D^{n'-k}_{k,j} \qquad (3\text{-}36)$$

In order to further simplify the notation and additionally, since we wish to concentrate on the end effect in the (z,t') plane, we will write the second space differencing in x of equation (3-32 c) as

$$\begin{bmatrix} \delta_x^2 & U_{k,1}^{n'} \\ \delta_x^2 & U_{k,2}^{n'} \\ \vdots & \\ \delta_x^2 & U_{k,J}^{n'} \end{bmatrix} = - \frac{T\, U_k^{n'}}{(\Delta x)^2} \qquad \text{for} \quad j=1,2,\ldots,J \qquad (3\text{-}37)$$

where T is a tridiagonal matrix with the elements $(-1, 2, -1)$ along the diagonal. Thus, in terms of vectors $U_k^{n'}$ and $D_k^{n'}$ along the x-coordinate, equation (3-36) may be expressed as

$$(1-Z)(1-W)\, U_k^{n'} = (1+Z)(1+W)\; aT\; U_k^{n'} + 1/2(1-Z)(1+W)\; C_k\, D_k^{n'-k} \qquad (3\text{-}38)$$

Let us now define an upward source term which is the shifted downgoing wave multiplied onto the reflection coefficients

$$S_k^{n'} \triangleq C_k\, D_k^{n'-k} \qquad \text{for} \quad n' > k \qquad (3\text{-}39)$$

In terms of source waves, equation (3-38) becomes

$$(1-Z)(1-W)\, U_k^{n'} = (1+Z)(1+W)\; aT\; U_k^{n'} + 1/2(1-Z)(1+W)\; S_k^{n'} \qquad (3\text{-}40)$$

and, rearranging, we have the matrix equation

$$[I-aT](1+ZW)\, U_k^{n'} - [I+aT](Z+W)\, U_k^{n'} - 1/2(1-Z)(1+W)\, S_k^{n'} = 0 \; . \qquad (3\text{-}41)$$

Likewise, the finite difference approximation to equation (3-31 b) for the downgoing waves is

$$\frac{\delta_{t''}\delta_z}{\Delta t\, \Delta z}\, D_{k,j}^{n''} = \frac{\tilde{v}}{2(\Delta x)^2}\, \delta_x^2\, D_{k,j}^{n''} \qquad (3\text{-}42)$$

Using the centered difference approximations of (3-32 a,b) we have

$$\frac{(1-Z)(1-W)}{(1+Z)(1+W)} \; D^{n''}_{k,j} \;=\; a\,\delta_x^{\,2}\, D^{n''}_{k,j}$$

$$(1-Z)(1-W)\; D^{n''}_{k} \;=\; -\,(1+Z)(1+W)\;\; aT\;\; D^{n''}_{k}$$

$$[I+aT](1+ZW)\; D^{n''}_{k} - [I-aT](W+Z)\; D^{n''}_{k} \;=\; 0 \qquad (3\text{-}43)$$

Let us now examine the (z,t') plane of the upcoming wave field. Recall that the x-coordinate has been absorbed in the matrix notation and it is therefore important to keep in mind the implicit third dimension in the calculations. Each cell in Figure 3-2 represents an end-view of the wave field looking along the x-axis. The column of cells at $k=0$ $(z=0)$ is the upcoming wave at the surface. By our definition, this is the reflection seismogram $R(x,t)$ recorded with receivers at the surface. The other point of interest is the diagonal line of cells representing the first arrival trajectory in (z,t') of a downgoing wave exiting the surface at $t=t''=0$. Above this diagonal the upcoming waves must vanish since a reflected wave cannot exist prior to the first arrival of the downgoing wave. This is incorporated in the initial conditions for the upcoming waves in equation (3-31 e). The region of interest for the source wave field S is similarly restricted to the same triangle. Prior to the first downgoing arrival $n' < k$, $S^{n'}_k = C_k\, D^{n'-k}_k \equiv 0$. At the surface we will require that the sources vanish, i.e., $C_0 \triangleq 0$ since reflections at the free surface are

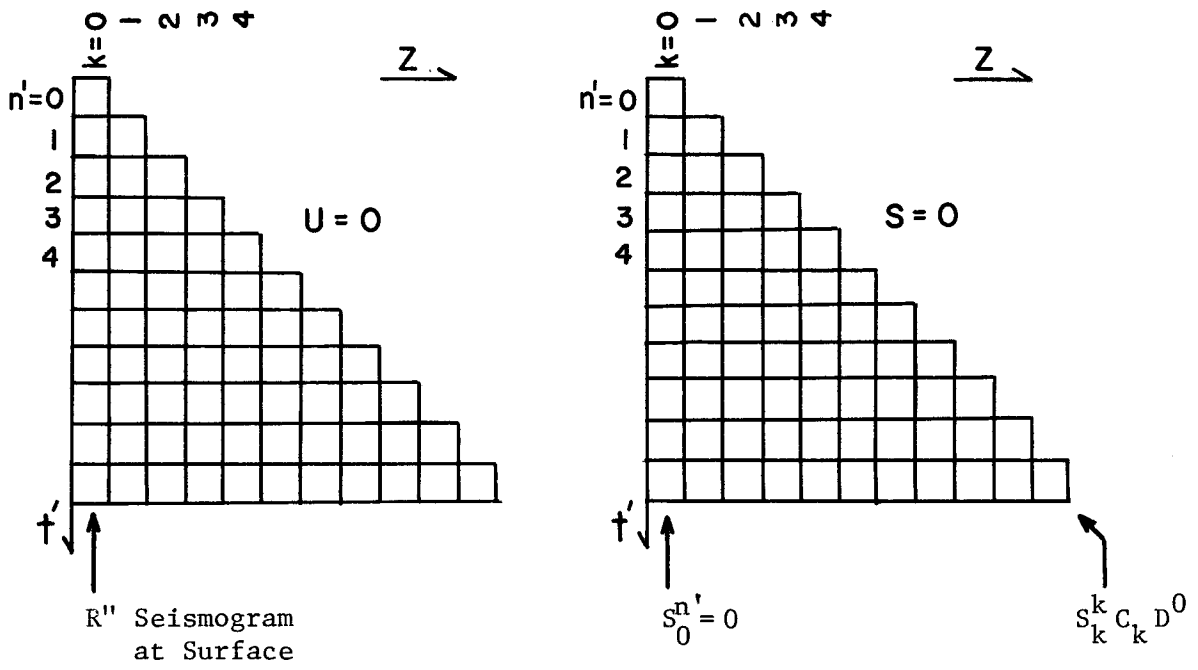

Figure 3-2. Upcoming and source wave fields observed in the (z,t') plane. Normal to this plane is the x (profiling axis). The upcoming wave equation propagates waves across the inner triangular region up to the surface. Above the diagonal both U and S vanish prior to the first downgoing arrival $t''=0$ $(n'=k)$. The reflection seismogram is defined as the upcoming wave field observed at the surface.

handled separately by the boundary condition (3-31 c). Along the first arrival trajectory $n'=k$ primary reflected waves are generated by the interaction of D_k^0 with the reflection coefficients. Thus, all multiple reflections originate due to sources inside the triangle $S_k^{n'}$, $0 < k < n'$; i.e., from downgoing waves exiting the surface at times $t'' > 0$.

The upcoming and downgoing wave propagators of equations (3-41) and (3-43) may be thought of as two-dimensional (matrix) convolution operators or filters acting on four neighboring cells in the (z,t') plane of U, S and in (z,t'') of D , respectively. Identifying W as a unit backward-shift in z and Z as a unit time-delay, equation (3-41) may be represented as

$$\begin{array}{c} z \rightarrow \\ t'' \downarrow \end{array} \quad \begin{array}{c|cc} & k & k+1 \\ n' & (I-aT) & -(I+aT) \\ n'+1 & -(I+aT) & (I-aT) \end{array} \circledast U \; - \; \begin{array}{c|cc} & k & k+1 \\ n' & -1/2 & -1/2 \\ n'+1 & 1/2 & 1/2 \end{array} \circledast S = 0 \qquad (3\text{-}44)$$

The symbol $\circledast$ denotes the two-dimensional matrix convolution where the 2×2 operators are laid-down on corresponding cells in the U and S (z,t') planes. Similarly, equation (3-43) may be represented as the operator

$$\begin{array}{c} z \rightarrow \\ t'' \downarrow \end{array} \quad \begin{array}{c|cc} & k & k+1 \\ n'' & -(I+aT) & (I-aT) \\ n''+1 & (I-aT) & -(I+aT) \end{array} \circledast D = 0 \qquad (3\text{-}45)$$

acting in the (z,t'') plane of the downgoing wave.

Depending on the direction of the calculation there are four possible unknowns that may be solved for or directions to move with either (3-44) or (3-45). For example, knowing S and the cells $U_k^{n'}$, $U_k^{n'+1}$, and $U_{k+1}^{n'}$ we might attempt to determine $U_{k+1}^{n'+1}$ by solving

$$[I-aT]\, U_{k+1}^{n'+1} = [I+aT]\left(U_{k+1}^{n'} + U_k^{n'+1} \right) - [I-aT]\, U_k^{n'} + 1/2\left(S_k^{n'+1} + S_{k+1}^{n'+1} - S_{k+1}^{n'} - S_k^{n'} \right) \tag{3-46}$$

However, as Claerbout and Johnson (1971) point out such a direction is definitely unstable, similar to attempting polynomial division with a non-minimum-phase polynomial. This is also the case for $U_k^{n'}$ unknown. This mathematical predicament is a result of violating causality by attempting to propagate a wave in an unnatural direction. That is, the differential equation (3-31 a) and its approximation (3-44) are valid only for propagating waves upward when time runs forward. It is therefore not surprising that, with equation (3-46) trying to push upcoming waves downward while time runs forward, we should encounter numerical problems.

There are two allowable directions for the computations to proceed for both the upcoming and downgoing operators. They are directions in which the unknowns are multiplied onto the matrix $[I+aT]$, guaranteed stable numerically and causal physically; specifically:

$U_k^{n'+1}$, $D_{k+1}^{n''+1}$ (with time going forward) and

$U_{k+1}^{n'}$, $D_k^{n''}$ (with time going backwards).

In the forward problem we restrict interest to propagation in the $+t$ sense.

In order to best illustrate the steps involved in the forward calculation, let us consider in detail one cycle in the algorithm. Assume that the model C is prescribed for all space, and the surface disturbance E is given. Assume that the seismogram R has been computed out to and including $n = 3$. Referring to Figure 3-3 the free surface boundary condition gives us the values for the cells at the left-hand $(z=0)$ side of the downgoing grid. With the operator (3-45) we may downward continue these waves from surface cells $(E , d_0^1 , d_0^2 , d_0^3)$ to fill out the grid. The next step is to shift the time axis t'' into the t' frame as per $t' = t'' + 2z/\tilde{v}$ or in sample space $n' = n'' - k$. This downgoing wave, referenced in the upcoming system is then cross-multiplied onto the known reflection coefficient $(c_1, c_2, c_3, c_4, \ldots)$ cells generating the upward source terms $S_k^{n'}$.

These reflected waves are finally upward continued to the surface with the operator (3-44) and the new row (cell r_4) is developed on the reflection seismogram. The cycle continues by reinserting this surface arrival, after an appropriate 180° phase shift, back into the downgoing calculation.

Thus, expressing the initial-boundary value problem of equations (3-31) in terms of finite differences yields the following numerical algorithm for the forward calculation of two-dimensional reflection seismograms.

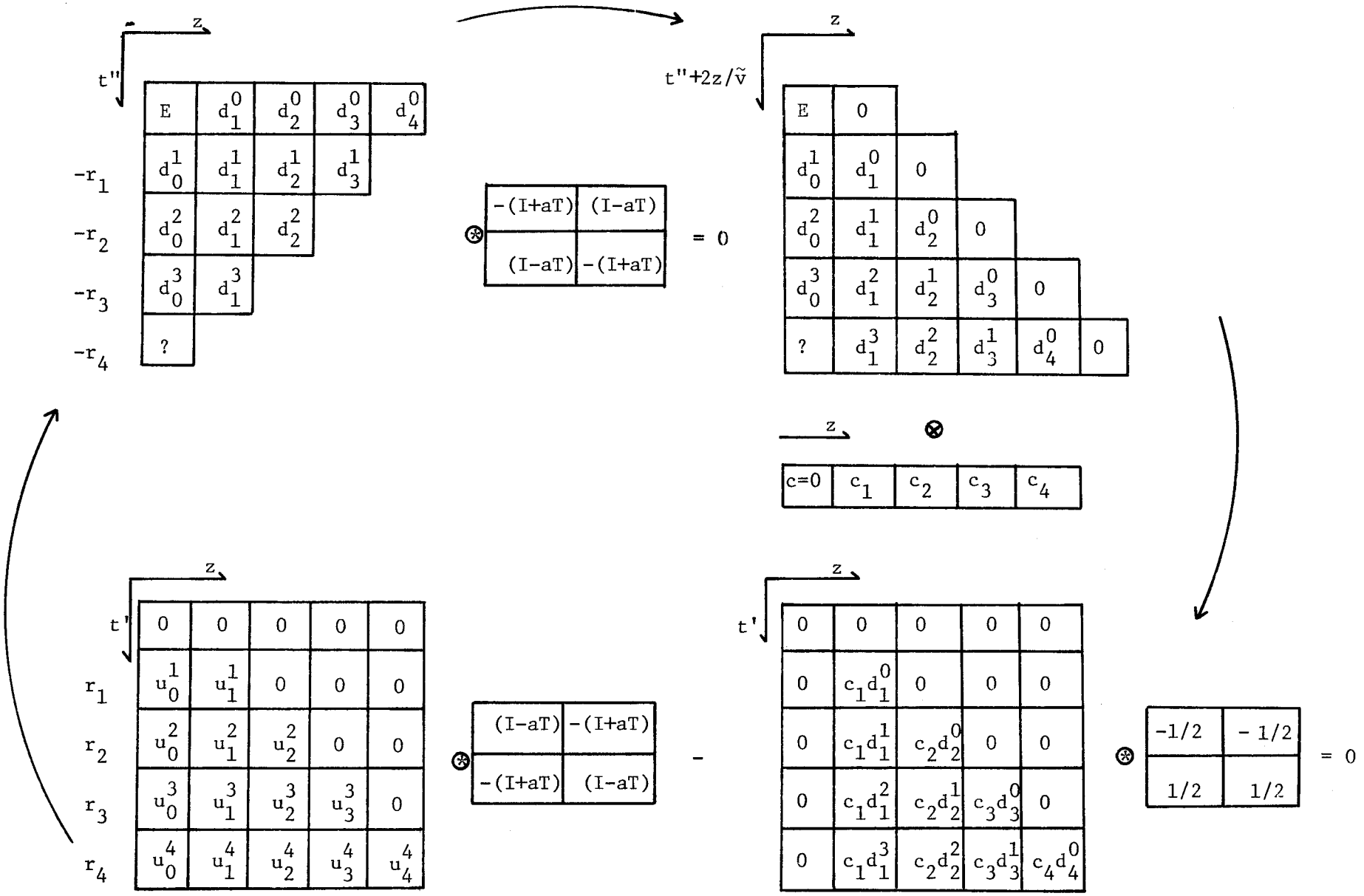

Figure 3-3. Illustration of one cycle in the forward algorithm. The figure is described in the text.

Initial cond:

$$U = 0 \text{ , all } n', k$$

$$D = 0 \text{ , all } n'', k \neq 0 \qquad \text{(3-47 a,b,c)}$$

$$D_0^0 = E$$

Difference eqns:

for $n' = 1, 2, 4, \ldots, n'_{max}$

for $n'' = 0, 1, 2, \ldots n'-1$ and $k = n' + n''$

$$[I+aT]D_k^{n''} = [I-aT](D_k^{n''-1} + D_{k-1}^{n''}) - [I+aT]\, D_{k-1}^{n''-1} \qquad \text{(3-47 d)}$$

for $k = n', n'-1, n'-2, \ldots, 0$

$$[I+aT]U_k^{n'} = [I-aT](U_{k+1}^{n'} + U_k^{n'-1}) - [(I+aT)]U_{k+1}^{n'-1} \qquad \text{(3-47 e)}$$

$$- 1/2(S_k^{n'} + S_{k+1}^{n'} - S_k^{n'-1} - S_{k+1}^{n'-1})$$

where $S_k^{n'} = C_k\, D_k^{n'-k}$

Boundary cond:

$$R^n = U_0^{n'} \qquad \text{(3-47 f,g)}$$

$$D_0^{n'} = -U_0^{n'}$$

2-D Gating Techniques

The number of numerical operations involved in propagating waves from the first arrival diagonal up to the surface is obviously proportional to the width or depth of the region spanned. Thus, as we move to later time on the seismograms we find ourselves faced with a growing computational procedure. For propagation through source free regions (with the homogeneous continuation equations) we may largely overcome this expense by taking large Δz steps. However, where we have non-zero reflectors interacting with non-zero portions of the downgoing wave we must proceed with Δz equal to model sampling rate $\frac{\tilde{v}\Delta t}{2}$. If we take a lead from the one-dimensional algorithm, we recognize that a certain amount of economizing gating may also be done for two dimensions. Therefore, we wish to delineate those areas in the (z,t') plane of S where we either know S to be zero or assume it to be negligible.

Certainly we have, in the forward problem, a priori knowledge about the $S(z,t')$ plane by prescribing the model. In modeling marine data we may identify the seafloor and use the fact that no reflectors exist in the water path to exclude some of the sources in (z,t') . Referring to Figure 3-4 we set $S_k=0$ for $k < N_{1S}$ where N_{1S} corresponds to the depth to the seafloor.

Next consider the short-diffraction-path multiples, i.e., those waves which eventually become trapped in the water layer. These include both returning deep reflections (short-diffraction-path peglegs) and simple seafloor multiples confined to the water path. If we gate-in the seafloor reflector, say bounded by $N_{1S} \leq k < N_{2S}$, we encompass all of the sources S necessary to model all multiples of

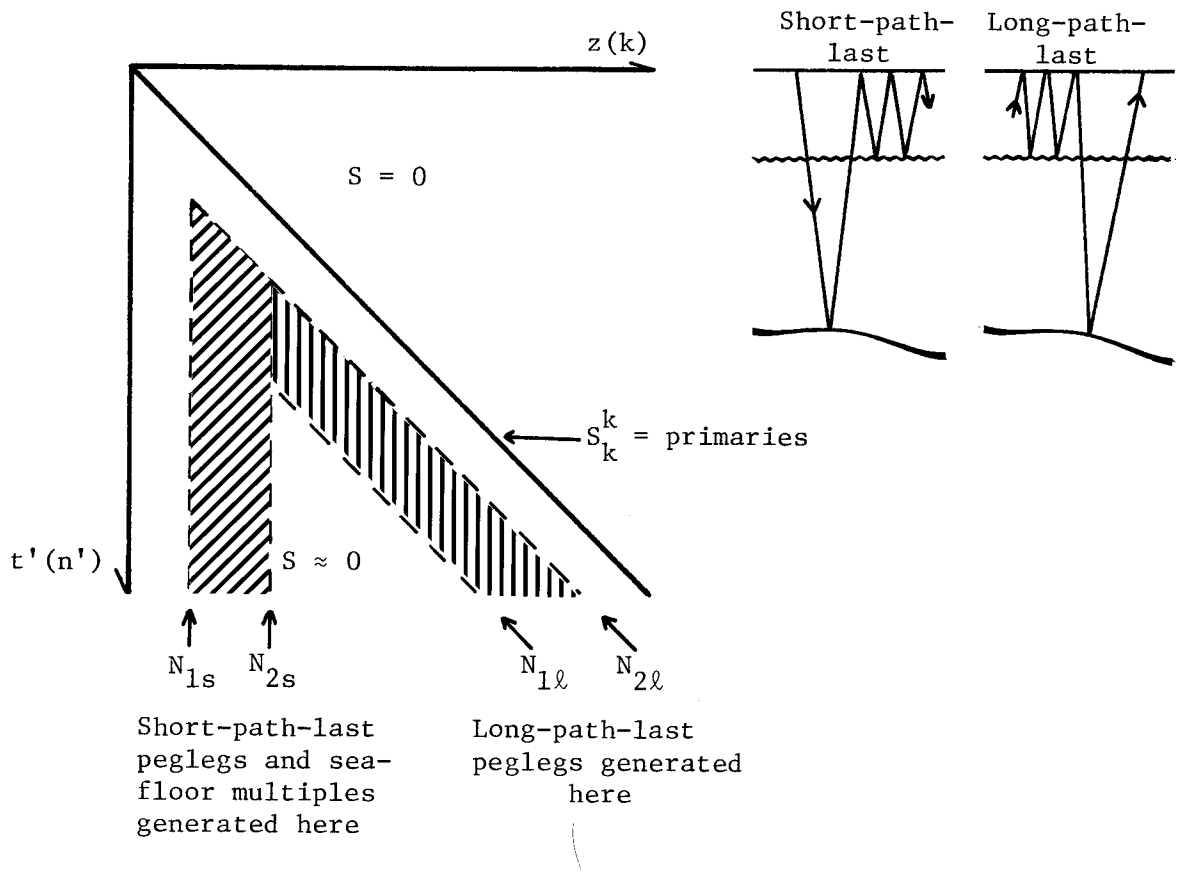

Figure 3-4. Gating arrangement in the (z,t') plane of S for discriminating between long and short-path multiples due to an initial plane wave source. $S_k = 0$ in the water path $k < N_{1s}$. Short-path-last structure peglegs and seafloor multiples are generated in the gate $N_{1s} < k < N_{2s}$. Long-path-last peglegs are generated by the interaction of the downgoing multiples with the structure reflectors. Thus, $S_k^{n'} \neq 0$ for $n' - N_{1\ell} < k < n' - N_{2\ell}$ where $N_{1\ell}$ and $N_{2\ell}$ encompass as much of the downgoing wave as might be considered significant. By delineating non-zero regions of the source plane $S(z,t')$ the homogeneous upcoming equation may be used with large Δz steps to propagate waves economically across source-free regions.

this class. On the other extreme we have the long-diffraction-path multiples. These include those waves which reverberate one or more times in the water layer prior to entering the subsurface. These are somewhat tricky to pin down on the (z,t') plane since this depends on the particular distribution of shots modeled. But for a plane wave source $E(x)=1$ the downgoing wave consists of the initial source at $t=t''=0$ followed by zeros until the first seafloor reflection exits the surface, $N_{1L}=N_{1S}$. Therefore we may exclude, for a plane source, S for $n'-N_{1L}< k < n'$. Recognizing a certain degree of arbitrariness, we may choose the long-diffraction-path gate N_{1L} to N_{2L} of figure 3-4 to encompass as much of the downgoing reverberations as might be considered significant. With this gating arrangement we approximately model the long-path class of multiples.

In the remaining inner triangular region structure-structure multiples are generated. For some practical situations we may be led to neglect these arrivals on the basis of amplitude. While the initial object of gating the calculation in the $S(z,t')$ plane was economy, we realize additionally the benefit of being able to selectively model those multiples of interest. That is, by modifying the S plane we may separate time coincident arrivals at the surface into distinct multiple classes. This separation will be illustrated in the numerical examples.

Synthetic Examples

In this section we will use the finite difference algorithm to simulate the 2-D reflection seismograms due to several reflector models. To begin with, the models are simplified to consist of point scatterers, and edge diffractors. Although the algorithm is valid for any number of complex-shaped reflectors, the simple models are best for illustrating and understanding diffracted multiple reflections. In any case the practical restriction is the wave angle.

For all but one example the calculations were made with a normally incident plane wave source $E(x)=1$. Additionally, the diffraction velocity was taken to be constant in each case. The simplest model which well illustrates all the free surface multiples consists of two spatially separated point reflectors. Referring to Figure 3-5, Frame (a) is the depth model with the ray paths drawn for the two pegleg paths. Since the incident source is a plane wave, the waves do not begin to diffract until the first reflection off of each point. Thus, the multiple path involving interaction with the deeper scatterer first (dashed lines) will undergo less diffraction relative to the other path. Due to this difference it becomes important to distinguish between two different types of pegleg multiples; short-path-last and long-path-last. Such a classification is valid for any order of pegleg reflections.

Frame (b) illustrates the arrival times for the primary paths and pegleg multiples as determined by tracing rays. Simple multiples involving just the free surface and a single scatterer were not traced. Their arrival times are identical to the primary hyperbola, displaced in time. Frame (c) is the actual model $C(x,z)$ that was used in the

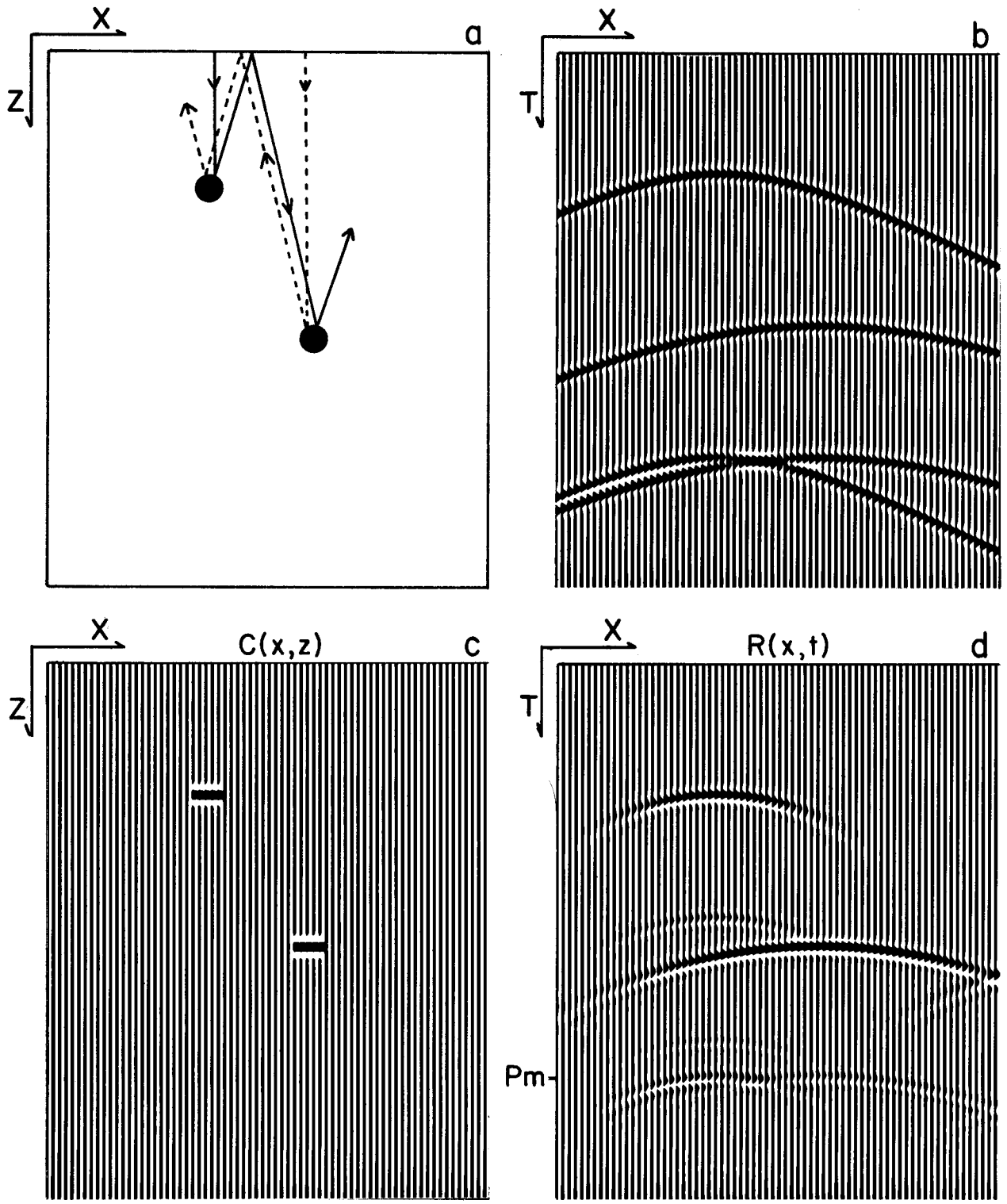

Figure 3-5. 2-D reflection seismogram of two point-diffractors in a constant velocity material due to a plane wave source. Frame (a): ray-paths for the long-path-last (solid line) and short-path-last (dashed line) pegleg multiples. Frame (b): ray travel-times for the primary and pegleg paths only. Frame (c): reflector model consisting of two point-diffractors of -1 reflectivity. Frame (d): computed 2-D reflection seismogram. The vertical is 1:1 , however due to the

Figure 3-5 Cont'd.
plane wave source all diffraction hyperbolas approach asymptote tangents of 0.5 instead of 1.0 for a point source. Waves propagating at angles greater than 30° were attenuated by numerical viscosity. This geometry best illustrates the separation of the arrivals for the two different peglegs (Pm). The long-path-last multiple (with travel-time minimum under the right scatterer) undergoes a longer diffraction path (hence less curvature on its hyperbola) relative to the short-path-last wave. The difference in diffraction curvature of the two paths is proportional to the vertical separation of the scatterers. Reflections off the rigid-wall boundary condition in x may be noted on the primary arrival of the deeper scatterer. Calculations of this size grid (70 x 350) take about a minute on an IBM 360/67.

calculation. Frame (d) is the 2-D reflection seismogram $R(x,t)$ calculated with the finite difference algorithm. In the calculation waves propagating at angles greater than 30° to the vertical were attenuated with numerical viscosity in the difference equations. This accounts for the tapering of the diffraction hyperbolas beyond this limit.

This calculation clearly illustrates the separation of the two types of peglegs at $t=P_m$. The long-path-last arrival, having a travel time minimum over the deeper scatterer, has been diffracted more and hence is represented by a broader hyperbola relative to the short-path-last arrival. The difference in curvature depends only on the vertical spearation of the points. Comparison between the ray-path travel times and the finite difference calculation is very good even out to 30°. Since more complicated reflector shapes may be constructed from point scatterers, frame (d) is the 2-D "impulse response" for diffracted multiple reflections due to two reflectors.

The next example is the situation of a flat seafloor overlying a point scatterer. Referring to Figure 3-6, frame (a) is the reflection coefficient model $C(x,z)$ used in calculating the seismograms. Frame (b) illustrates the two ray-paths for the first pegleg multiple. The long-path-last multiple (solid line) reverberates in the water layer without becoming diffracted. Entering the sub-bottom, it finally diffracts off the point reflector and is recorded at the surface as the narrow curvature hyperbola on the 2-D reflection seismogram $R(x,t)$ of frame (c). Directly beneath the scatterer the long and short paths are time-coincident and constructively interfere to produce the high amplitude arrival at the top of the pegleg hyperbolas. If the calculation had been continued to include the second order peglegs we would expect

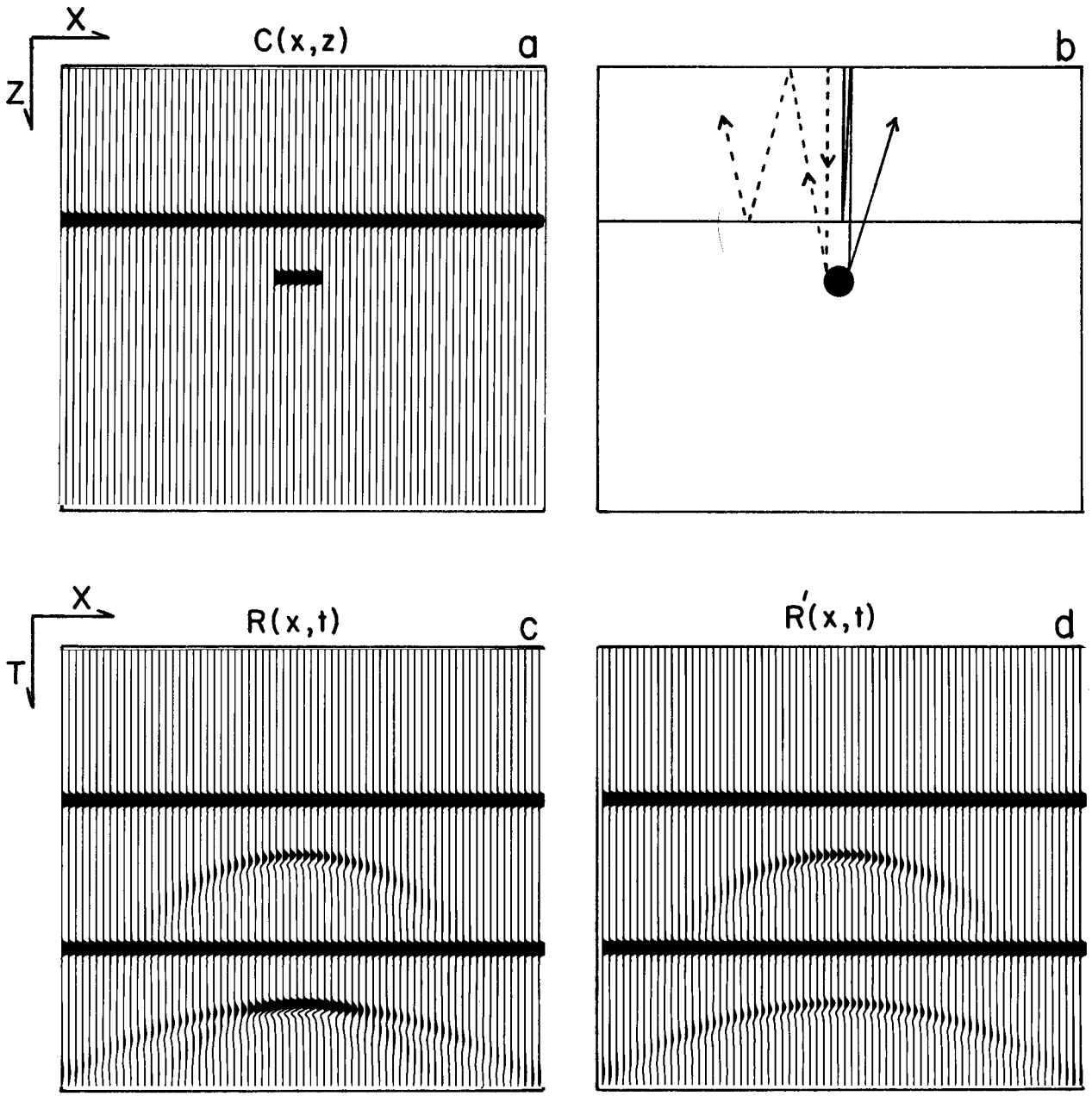

Figure 3-6. 2-D reflection seismogram for a plane, horizontal seafloor overlying a single point scatterer. The source is a plane wave and the diffraction velocity is constant. Frame (a): the reflector model used in the calculation. Frame (b): ray-paths for the primary and multiple reflected waves. The solid line is the long-path-last portion of the pegleg multiple while the dashed line represents the short-path-last arrival. Frame (c): the 2-D reflection seismogram R(x,t) calculated with the finite difference algorithm. In the lower third of the frame we record two distinct hyperbolas representing the difference in the amount of diffraction on the two pegleg paths. Beneath the scatterer the arrivals are time-coincident, constructively interfering to produce the high amplitude reflection. Frame (d) is R'(x,t) ; the seismogram calculated with the same model, however with the gating arrangement such that the long-path-last (narrow hyperbola) multiple was not computed. Again the vertical exaggeration is 1:1 .

to record three distinct hyperbolas with time-coincident tops.

Frame (d) illustrates the effect of gating the calculation in the (z,t') plane of S. The $N_{1s}-N_{2s}$ gate encompassed the horizontal seafloor and the calculation in the long-path-last gate $N_{1\ell}-N_{2\ell}$ was omitted. The resulting seismogram $R'(x,t)$ then only exhibits the short-path-last diffracted arrivals.

The opposite situation to the planar seafloor overlying a bumpy subsurface reflector (a point-diffractor being the extreme case) of Figure 3-6 is the geometry of a bumpy seafloor overlying a planar structure reflector. Here we again take the extreme of a "point seafloor". Referring to Figure 3-7, frame (a) is the reflection coefficient model, and frame (b) illustrates the long and short-path-last rays for this geometry. In this calculation structure-structure multiples (i.e., the simple multiple of the plane layer) were omitted by gating. Frame (c) is the reflection seismogram $R(x,t)$ computed including both pegleg paths. The stubby appearance of the long-path-last (solid ray) hyperbola is due to numerically attenuating waves outside the 30° beamwidth. Theoretically the long-path-last arrival of this model is identical to the short-path-last arrival of the previous model.

Frame (d) is the reflection seismogram $R'(x,t)$ due to the same model, however, excluding the long-path-last multiples by the same gating arrangement as for Figure 3-6 d. This represents the case of a returning primary wave reverberating once in the water layer. From these two models we are led to expect that the different diffraction path lengths represent distinct multiple processes in the presence of appreciable seafloor or structure topography. A wave transmitted a great distance into the earth, reflected back and trapped by the

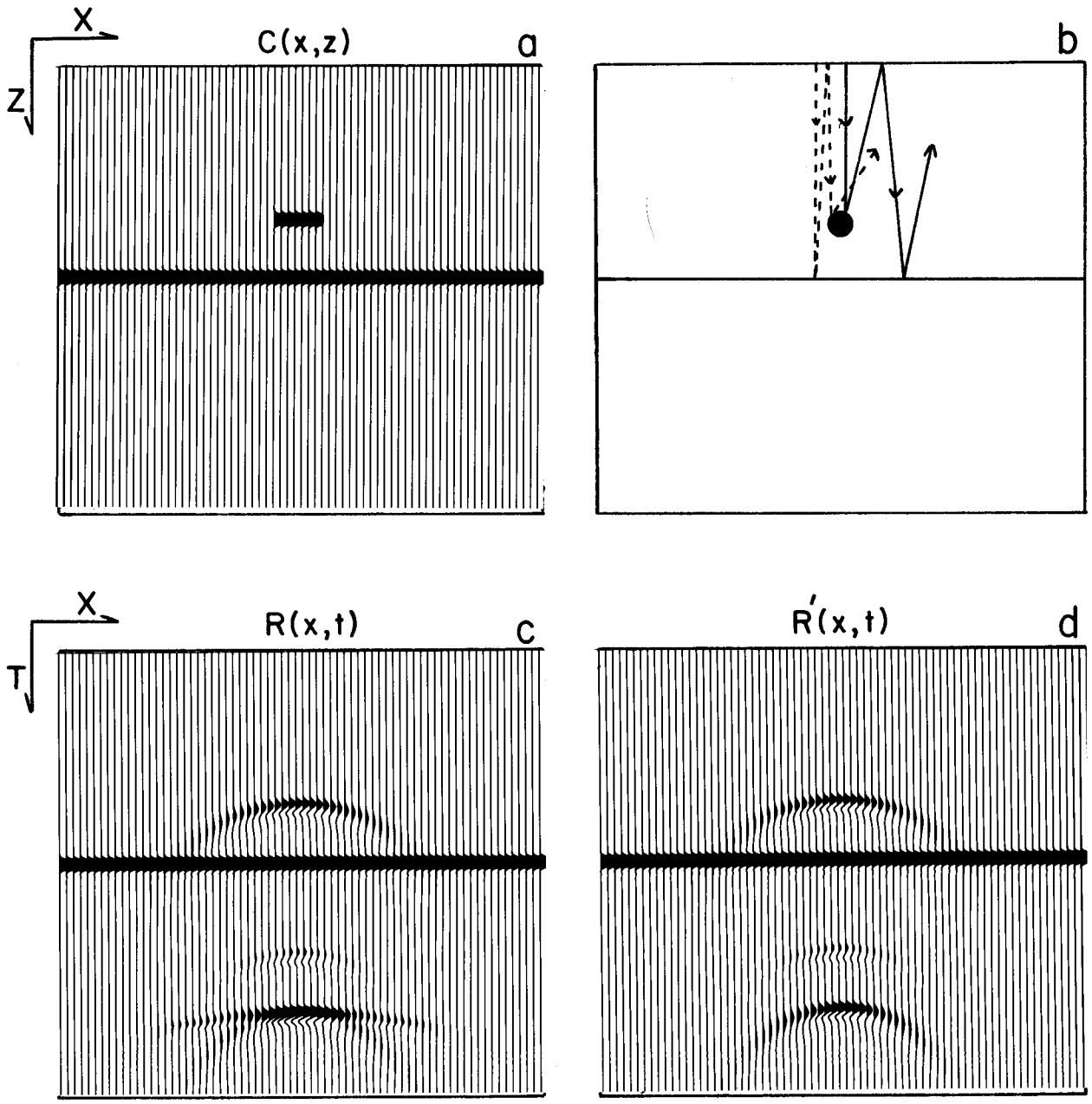

Figure 3-7. Reflection seismograms for a point-reflector overlying a plane layer. Normally incident plane wave source and constant diffraction velocity. Frame (a): the reflector model used in the finite difference algorithm. Frame (b): ray paths for the long(solid) and short-path-last (dashed) pegleg multiples. Frame (c): reflection seismogram R(x,t) including both pegleg arrivals. Gating the calculation accounts for the omission of the simple multiple of the plane layer. This represents the extreme case of a bumpy seafloor overlying a smooth structure reflector. Since waves at angles greater than 30° have been numerically filtered-out the long-path-last pegleg arrival appears truncated compared to the short-path-last multiple of Figure (3-6c). Theoretically they are identical, however in this geometry the waves approach the angular cutoff at smaller offset to the point scatterer. Frame (d) is the reflection seismogram computed excluding the long-path-last waves. The gating was identical to that used in Figure (3-6d). The vertical exaggeration is 1:1 .

water layer, would be successively stretched and scattered by the seafloor topography. However, depending on the relative depth of the seafloor and structure, this may amount to a small diffraction as compared to the situation where the wave gets deformed prior to the long travel path.

Figure 3-8 represents the case of a single plane interface offset by a vertical fault. Frame (a) is the reflection coefficient model and frame (b) is the computed seismogram due to a plane wave source. Note that the branches of the edge diffractions for both primary and simple multiple reflections undergo a polarity change crossing the top of the hyperbola. The back branches have the opposite polarity of the horizontal wave. As the fault displacement went to zero the diffraction would be extinguished. The pegleg arrival for this geometry consists of a single diffraction hyperbola midway between the simple multiples. Both pegleg paths have about the same total diffraction length and thus both arrive simultaneously at each receiver.

Frames (c) and (d) are the reflection seismograms for the same model, however the source was a point disturbance, $E(x) = \delta(x-s)$ at the surface, located to the left and right of the fault boundary. These frames then represent non-moveout-corrected single-shot profiles. The reason for the apparently wide pulse shape on the primary arrivals is the superposition of two hyperbolas of differing curvature. One is the normal moveout hyperbola of the flat interface reflection and the other is the diffraction (narrow curvature) hyperbola off the fault boundary. Due to the angular bandwidth of the shot numerous reflections off the rigid-wall conditions are recorded, especially on the multiple reflections.

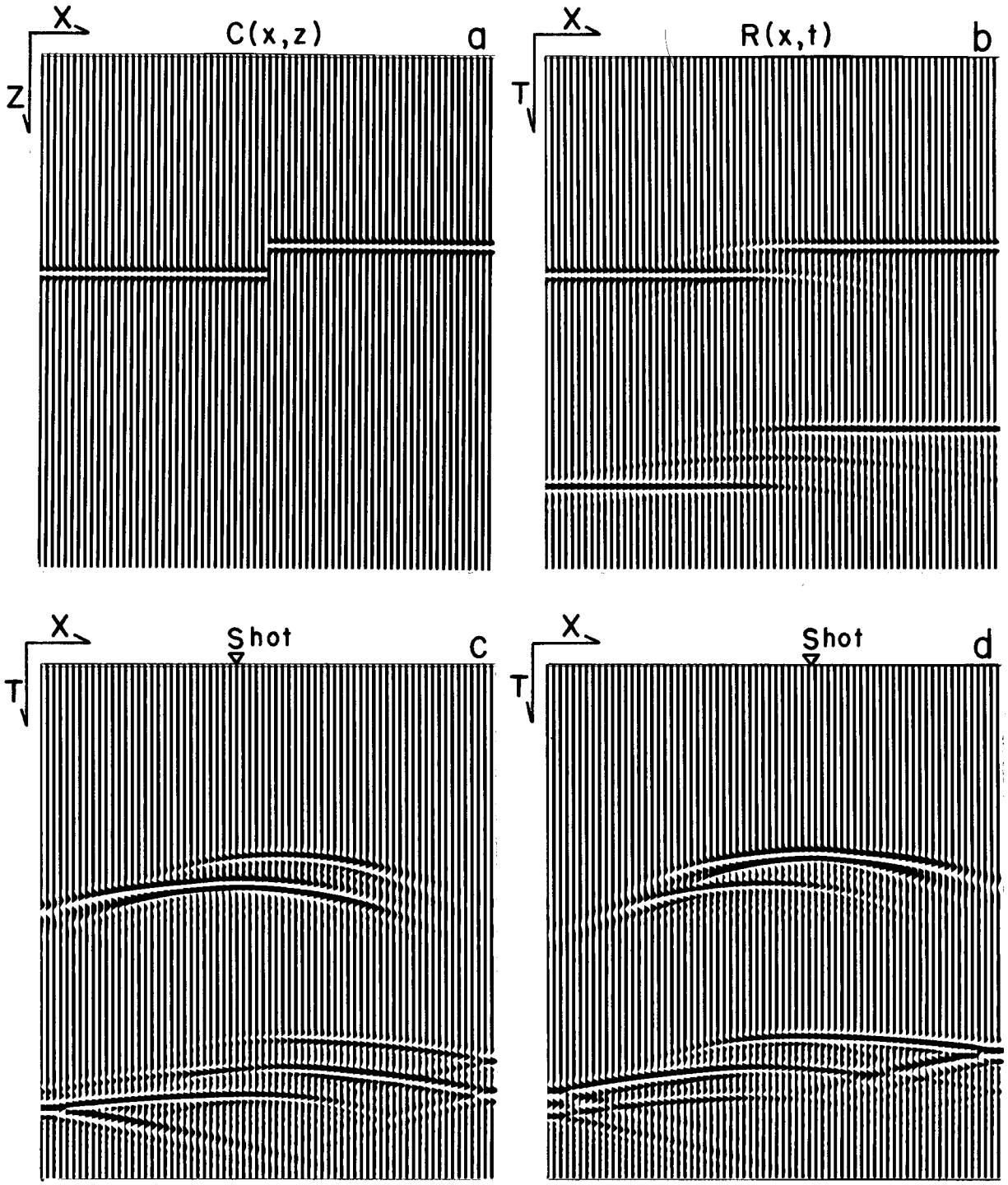

Figure 3-8. Reflection seismograms due to a vertically faulted plane interface. The vertical exaggeration is 1/2 on all frames. Frame (a): the reflector model C(x,z) consisting of a faulted plane layer. Frame (b) 2-D reflection seismogram including all free surface multiple reflections for an initial plane wave source and constant diffraction velocity. Characteristic of a 2-D edge diffraction is opposite polarity branches of the hyperbolic arrival times. The back branches of primaries and simple multiples have the opposite polarity of the horizontal wave. Since both

Figure 3-8 Cont'd.

pegleg paths have equal diffraction path length the pegleg arrival is a single hyperbola arriving midway between the simple multiples. All hyperbolas in frame (b) approach asymptote tangents of 1/4 . Frames (c) and (d) are the reflection seismograms for the same model, but due to an initial point source $E(x) = \delta(x-s)$. Normal moveout hyperbolas approximately overlap the edge diffraction hyperbolas (each having different curvature) accounting for the smeared pulse shape at wider offsets. Reflections off the rigid walls may be observed on the multiples in all three seismograms.

Figure 3-9 illustrates the geometry of an undulating seafloor overlying a deep, faulted, dipping layer. Frame (a) is the reflection coefficient model consisting of a seafloor of reflectivity 0.25 and faulted structure of strength -0.01 . For display purposes a uniform exponential gain of 36 db/sec. has been applied to both frames.

Frame (b) is the reflection seismogram computed for this model and a plane wave source. The simple seafloor multiples are successively stretched by the seafloor topography. The waves are focused in the troughs and diffused on the peaks. The degree of focusing is a function of seafloor curvature and increases uniformly from left to right. Note the diffraction hyperbolas of the structure primary due to scattering off the sharp fault boundaries.

Below the structure primary are the diffracted pegleg multiples. Due to the increasing multiplicity of paths, the subsequent arrivals decay at less than the exponential rate associated with the seafloor multiples. These multiples assume both the slope of the structure and the stretch of the seafloor topography. A large portion of the intense diffraction associated with the peglegs is due to the long-path-last (long-diffraction-path) arrival.

As a final example of the forward calculation, consider the case of a highly reflective, rough seafloor. In Figure 3-10 the seafloor model was a surface where the curvature or roughness increases away from the center of the section. The resulting seismogram illustrates diffracted seafloor multiples up to order 8. As the waves reverberate in the water layer they are successively stretched by the irregular seafloor topography. The more net stretch the faster the waves diffract. Thus, the multiple waves become increasingly focused in the seafloor troughs and diffused on the peaks. By the time of the fifth seafloor

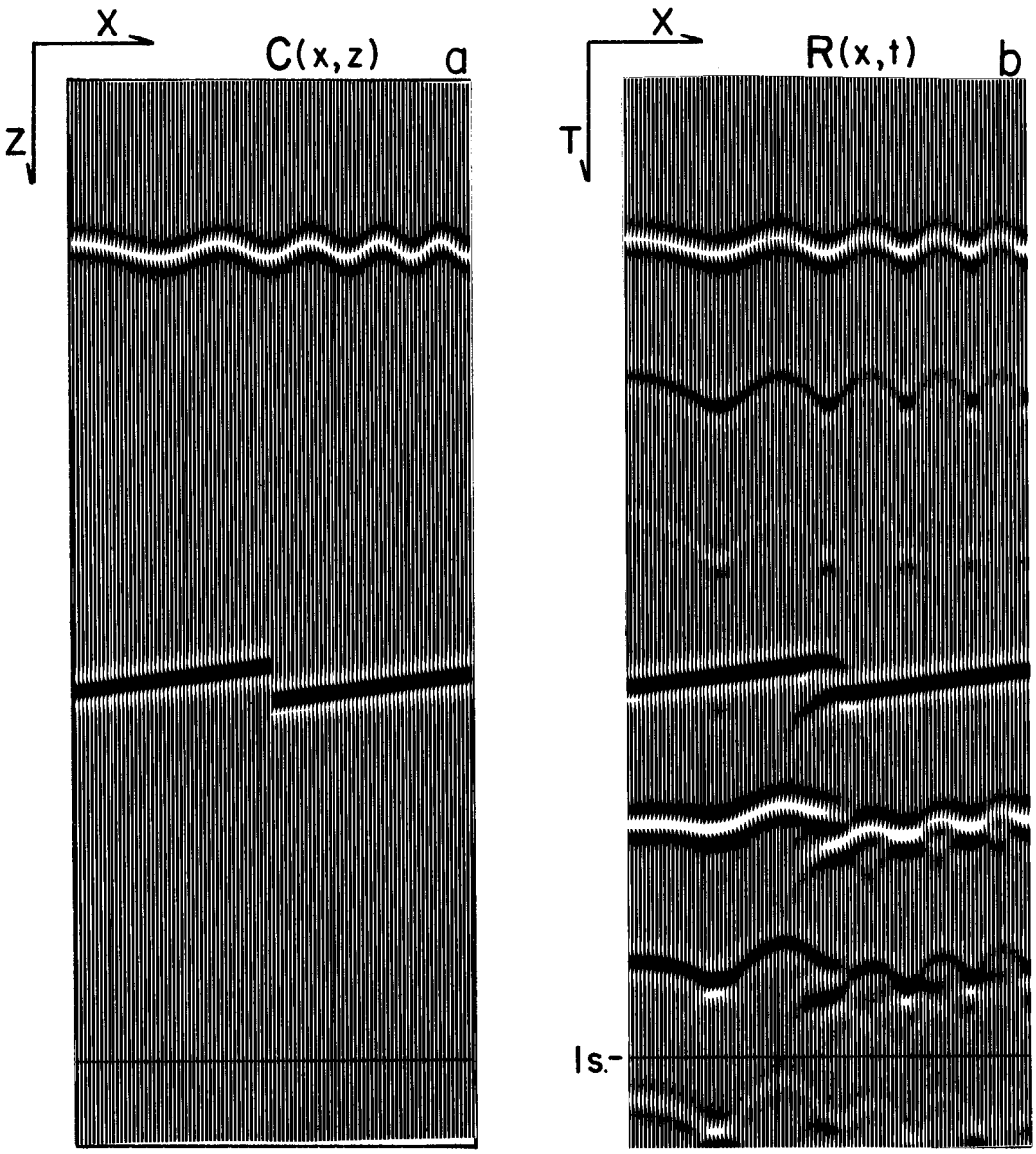

Figure 3-9. Undulating seafloor overlying a deep, faulted structure. Frame (a): the reflection coefficient model C(x,z) consisting of a chirp seafloor of 0.2 reflectivity and a dipping, faulted layer of strength -0.01 . For display purposes a uniform exponential gain of 36 db/sec was applied prior to plotting on both the model and reflection seismogram. Frame (b) is the reflection seismogram R(x,t) for an initial plane wave source. As the waves reflect in the water path they are successively stretched by the irregular seafloor. With each reflection the seafloor multiples become more focused in the trough and diffused on the peaks. The primary structure arrival exhibits the characteristic diffraction hyperbolas due to scattering off the fault boundaries. Below 0.75 sec. are the diffracted pegleg multiple reflections. Since there is an increasing number of possible path on successive pegleg arrivals they decay in strength somewhat slower than the exponential rate of the seafloor multiples. The vertical exaggeration is 5:1 .

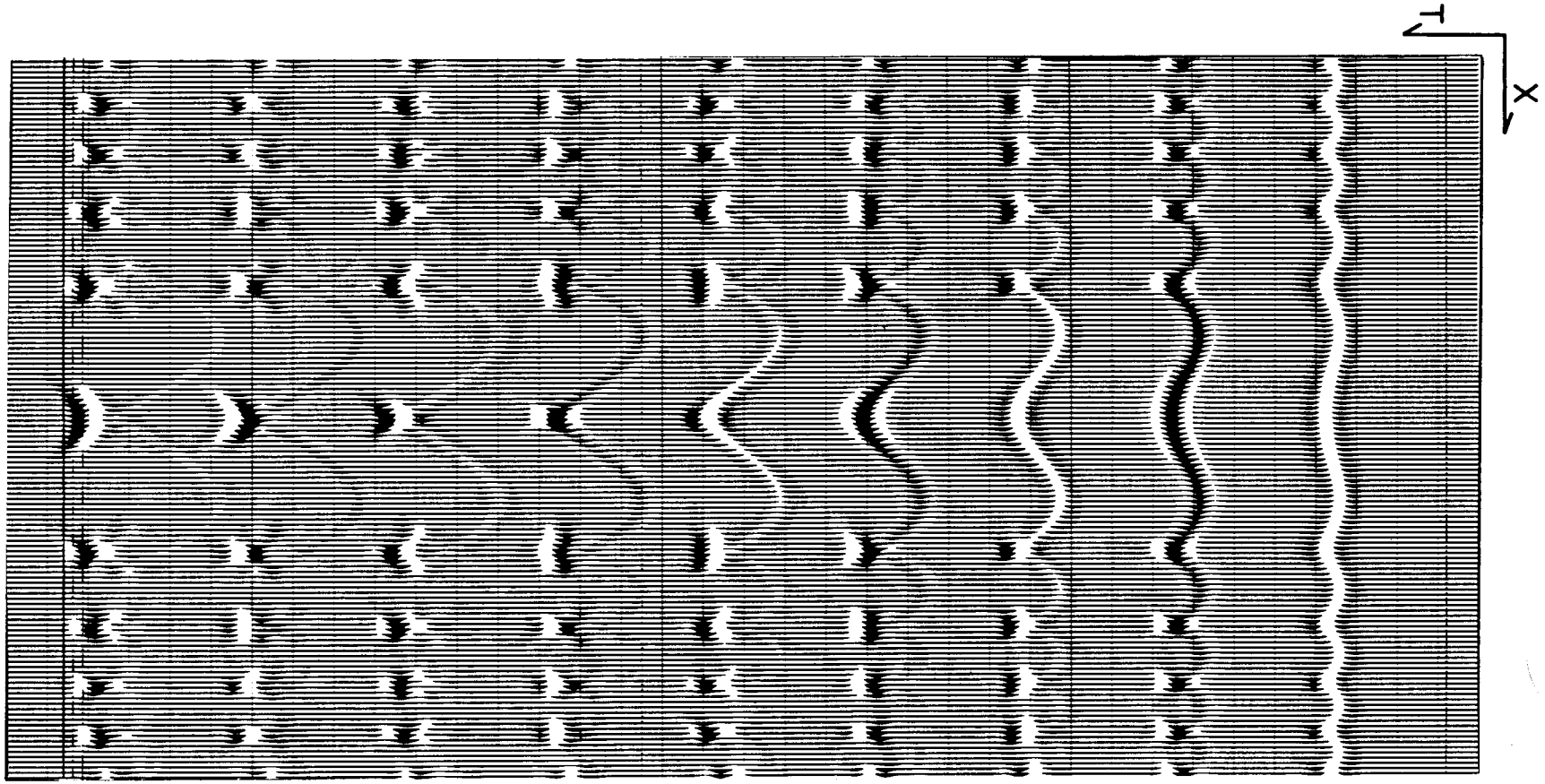

Figure 3-10. 2-D seafloor multiples due to a bumpy seafloor. Seafloor curvature, and hence diffraction, increases away from the center of the figure. Below the topographic lows the waves focus; below the highs the waves are diffused. Even for moderate seafloor relief, successive focusing and defocusing leads to lateral incoherence on the high order multiples. This example was computed by Jon F. Claerbout.

multiple the process of focusing and defocusing adjacent portions of the wave leaves almost no lateral coherence toward the edges of the section. This illustrates the fact that even for moderate seafloor topography there may be dramatic wave effects on the high-order multiples.

An important conclusion that we may draw from these examples of the forward calculation relates to mapping subsurface reflectors. Where we have two-dimensional structure there is the possibility of recording diffracted multiple reflections, arriving in near time-coincidence, having different curvature hyperbolas. Thus, it is impossible to reduce two-dimensional multiples to one-dimensional multiples by a single migration operation. Multiples, in general, may not be migrated as primaries. With this fact in mind, we may expect to encounter difficulty in applying the time-honored 1-D principle of time coherence as a means of identifying and removing 2-D multiple reflections. A consistent mapping of reflectors, including the information contained in the multiples, must involve migration occurring simultaneously with the prediction and elimination of multiple reflections.